Examination of the Topographical Anatomy and Fetal Development of the Tendinous Annulus of Zinn for a Common Origin of the Extraocular Recti

Tetsu Naito,[1] Kwang Ho Cho,[2] Masahito Yamamoto,[1] Hidetomo Hirouchi,[1] Gen Murakami,[1,3] Shogo Hayashi,[4] and Shinichi Abe[1]

[1]Department of Anatomy, Tokyo Dental College, Tokyo, Japan
[2]Department of Neurology, Wonkwang University School of Medicine and Hospital, Institute of Wonkwang Medical Science, Iksan-si, Jeollabuk-do, Republic of Korea
[3]Division of Internal Medicine, Jikou-kai Clinic of Home Visits, Sapporo, Japan
[4]Department of Anatomy, School of Medicine, International University of Health and Welfare, Narita, Japan

Purpose. The aim was to clarify the topographical anatomy of the common tendinous ring for the four rectus muscles in both adults and fetuses.

Methods. We histologically examined the annular ligament for a common origin of the extraocular rectus muscles using 10 specimens from elderly individuals and 31 embryonic and fetal specimens.

Results. At 6 to 8 weeks, each rectus carried an independent long tendon, individually originating from the sphenoid. Notably, we found additional origins from the optic or oculomotor nerve sheath. At 12 to 15 weeks, the lateral, inferior, and medial recti muscles were united to provide a C-shaped musculofibrous mass that was separated from the superior rectus originating from the edge of the optic canal opening. Morphologic features at 31 to 38 weeks were almost the same as those at 12 to 15 weeks, but the long and thick common tendon of the three recti reached the sphenoid body in the parasellar area. In adults, a ring-like arrangement of the rectus muscles ended at a site 8.1 to 12.0 mm anterior to the optic canal opening and independent of the superior rectus origin, the lateral, inferior, and medial recti formed a C-shaped muscle mass. The united origins of the three recti changed to a fibrous band extending along the superomedial wall of the orbital fissure.

Conclusions. Consequently, none of the specimens we examined exhibited an annular tendon representing a common origin of the four recti, suggesting that the common tendinous ring includes only medial, lateral, and inferior rectus muscles with the superior rectus taking its origin independently.

Keywords: annular ligament, annulus of Zinn, common tendinous ring, extraocular recti, superior orbital fissure, optic canal, human fetus

The annular ligament representing a common origin of the four extraocular rectus muscles (anulus tendineus communis Zinni) encloses the optic nerve and ophthalmic artery as well as the oculomotor, nasociliary, and abducens nerves. According to *Morris' Human Anatomy*,[1] the tendinous ring (1) unites firmly with the dural sheath of the optic nerve and (2) contains two heads of the lateral rectus, sandwiching nerves that pass through the orbital fissure. Unfortunately, it appears that there are no photos showing the origins of the four rectus muscles from the tendinous ring. Koornneef[2,3] demonstrated a frontal section near the adult orbital apex, but his photos did not include the tendinous ring. However, Koornneef[2] and Sevel[4] described that, at 8 weeks, the medial rectus fuses with the dural sheath of the optic nerve, and that even at this early stage it is stronger and more fully developed than the lateral rectus. Sevel[4] also described the origins of the recti from the perichondrium at the orbital apex. Is it possible that the dural

or perichondral origin of the recti changes to a common tendinous origin at a later stage?

Although it is rare and highly site-specific, striated muscle origin from or insertion to the dura mater is a recent interest for anatomists and neurosurgeons (reviewed by Kahkeshani and Ward[5]). In their excellent and comprehensive embryological review, Tawfik and Dutton[6] considered the issue of whether or not a dural origin remains constant to be controversial. In human fetuses, we have reported temporal or transitory muscle insertion to a nerve sheath at two sites: (1) a developing tendon of the obturator internus muscle to the sciatic nerve[7] and (2) a developing tendon of the digastricus muscle posterior belly to the hypoglossal nerve.[8] Therefore, during fetal development, the origin of the extraocular recti is also likely to change from a nerve sheath (possibly, not the dura) to a cartilage or bone. Consequently, the aim of the present study was to clarify the topographical anatomy of the common tendinous ring for the

four rectus muscles in cadaveric material from both adults and fetuses.

MATERIALS AND METHODS

The study was performed in accordance with the provisions of the Declaration of Helsinki (as revised in Edinburgh 2000). We examined histological sections from 31 paraffin-embedded embryos and fetuses (6–38 weeks of gestational age [GA]), as well as 10 adult specimens.

The adult specimens were obtained from 10 cadavers (four males and six females, aged 76–97 years at the time of death). The cause of death was ischemic heart failure or intracranial bleeding. These cadavers had been donated to Tokyo Dental College for research and education on human anatomy, and their use for research had been approved by the university ethics committee. The donated cadavers had been fixed by arterial perfusion with 10% vol/vol formalin solution and stored in 50% vol/vol ethanol solution for more than 3 months. From each cadaver, we prepared tissue blocks (mostly 20 mm^3) including the orbital apex and sphenoid body. The specimens were decalcified by incubating them at room temperature in Plank-Rychlo solution (AlCl$_2$/6 H$_2$O, 7.0 wt/vol%; HCl, 3.6; HCOOH, 4.6) for 1 to 2 weeks. After routine procedures for paraffin embedding, we prepared frontal or sagittal sections (frontal for six cadavers and sagittal for four cadavers; 10-μm thick at 100–200-μm intervals) and stained them with hematoxylin and eosin (HE).

The embryonic or fetal specimens were classified into three stages: nine embryos and early fetuses at GA 6 to 8 weeks (crown-rump length [CRL] 21–38 mm), 12 midterm fetuses at GA 12–15 weeks (CRL 85–118 mm) and 10 fetuses near term at GA 31–38 weeks (CRL 260–310 mm). The paraffin blocks contained all parts of the head and neck at the early and midterm stages, whereas the specimens near term contained a left or right half of the head above the palate. All specimens were part of the large collection kept at the Embryology Institute of the Universidad Complutense, Madrid. The specimens were obtained from the University's Department of Obstetrics and were the products of miscarriages and ectopic pregnancies. The university ethics committee approved the study (B08/374). After routine procedures for paraffin-embedded histology, serial 7-μm-thick sections were cut frontally for 21 embryos and fetuses at the early and midterm stages. Because of the large size of the specimens from the 10 fetuses near term, however, sections 10-μm thick were cut at intervals of 50 to 100 μm. For all specimens, most sections were stained with HE, but a minor proportion were stained with azan or silver impregnation. Most photographs were taken with a Nikon (Tokyo, Japan) Eclipse 80, whereas photographs at ultra-low magnification (objective lens less than ×1) were obtained using a high-grade flat scanner with translucent illumination (Epson [Suwa, Japan] scanner GTX970).

RESULTS

Observations of Embryonic and Fetal Sections

Early Stage. In the nine specimens at 6 to 8 weeks (Fig. 1), because the eye faced the lateral aspect of the head, the frontal planes provided longitudinal or oblique sections of the extraocular recti (Figs. 1A–E). However, when the planes were tilted, we obtained sections showing a circular arrangement of the four recti (Fig. 1F). In these tilted planes (Figs. 1F, 1G), the optic nerve entered the orbit through a large gap between the superior (SR) and medial rectus muscles (MR). Posterior to the optic nerve entrance, the lateral rectus (LR), inferior rectus (IR), and MR were connected mutually to form a C-shaped fibrous

mass (Fig. 1G). In contrast, in the plane showing longitudinal sections through the recti, we found that each muscle possessed an independent long tendon originating from a small process on the sphenoid (Figs. 1B, 1C). Notably, in addition to this tendinous origin, we found that parts of the SR and/or LR fibers originated from the optic or oculomotor nerve sheath (Figs. 1A, 1D).

Midterm. In the 12 fetuses at 12 to 15 weeks (Fig. 2), the optic nerve passed superomedially between the SR and MR to enter the optic canal, which had begun to ossify (Figs. 2A, 2F), changing gradually in appearance of the cartilage to near term. Without an independent long tendon, the superior rectus originated from the upper edge of the optic canal, opening anterosuperiorly to the origins of the other three muscles (Figs. 2A, 2G). Therefore, more posterior sections did not contain the SR. At the anteroposterior level of the optic canal opening, the MR, IR, and LR were united to provide a C-shaped musculofibrous mass partly surrounding the oculomotor nerve at the center of the "C" (Figs. 2A, 2G). Notably, these three united rectus muscles changed to a thick fibrous bundle (or a common tendon) and extended posteriorly to reach the parasellar area (Figs. 2C, 2I). At a margin of the future cavernous sinus, the apparently common tendon ended at a process on the sphenoid body at an anteroposterior level including the maxillary nerve at a margin of the future cavernous sinus (Fig. 2D) or, more anteriorly, near the optic canal entrance (Figs. 2H, 2I).

Late-Stage Near Term. In the 10 fetuses at 31 to 38 weeks (frontal sections in Fig. 3 and sagittal sections in Fig. 4), hard tissues of the orbital apex as well as the posterior part of the orbital floor had not yet become established. Frontal sections demonstrated morphologic features similar to those at midterm: (1) independent of the MR, IR, and LR, the SR originated from the superomedial edge of the optic canal opening (Figs. 3C, 3G), (2) the other three recti were united to form a C-shaped mass (Figs. 3D, 3I), and (3) the tendinous common origin of the three recti extended posteriorly through the future orbital fissure and ended at the sphenoid body in the parasellar area (Fig. 3J), or, more anteriorly, near the optic canal entrance (Fig. 3E). The individual variation in origin was the same as seen in midterm fetuses (Fig. 2D versus Fig. 2I).

Notably, although the number of specimens was limited to four, sagittal sections demonstrated a consistent thin slip or minor head of the MR originating from the anterosuperior edge of the optic canal opening immediately posterior to the obliquus superior (SO; Fig. 4B). Thus, the MR carried an additional origin that was independent of the C-shaped common muscle mass of the three recti. The thickness of the additional head was less than one-third that of the major muscle slip of the MR. Along the upper margin of the canal opening, the levator palpebrae superioris (LPS) originated from a site between the origins of the SR and SO. Thus, the LPS origin appeared to connect among the origins of the SR, SO, and the additional head of the MR. Moreover, the origins of the LPS, SO, and the additional head of the MR had no definite tendinous material but muscular. In sagittal sections, the common tendinous origin of the MR, IR, and LR ended at the sphenoid on the anterior margin of the parasellar area (Figs. 4A, 4B). The oculomotor nerve passed through a narrow gap between the sphenoid and the common tendon (Figs. 4D, 4E). The optic nerve ran from the bottom of the U-shaped arrangement of the SR, LR, and IR to the eyeball (Figs. 4F–4H). If the MR was added three-dimensionally, a U-shaped arrangement was recognizable.

Observations of Sections From Adults

A ring-like arrangement of rectus muscle bellies enclosed the optic, abducens, oculomotor, and nasociliary nerves (Fig. 5A).
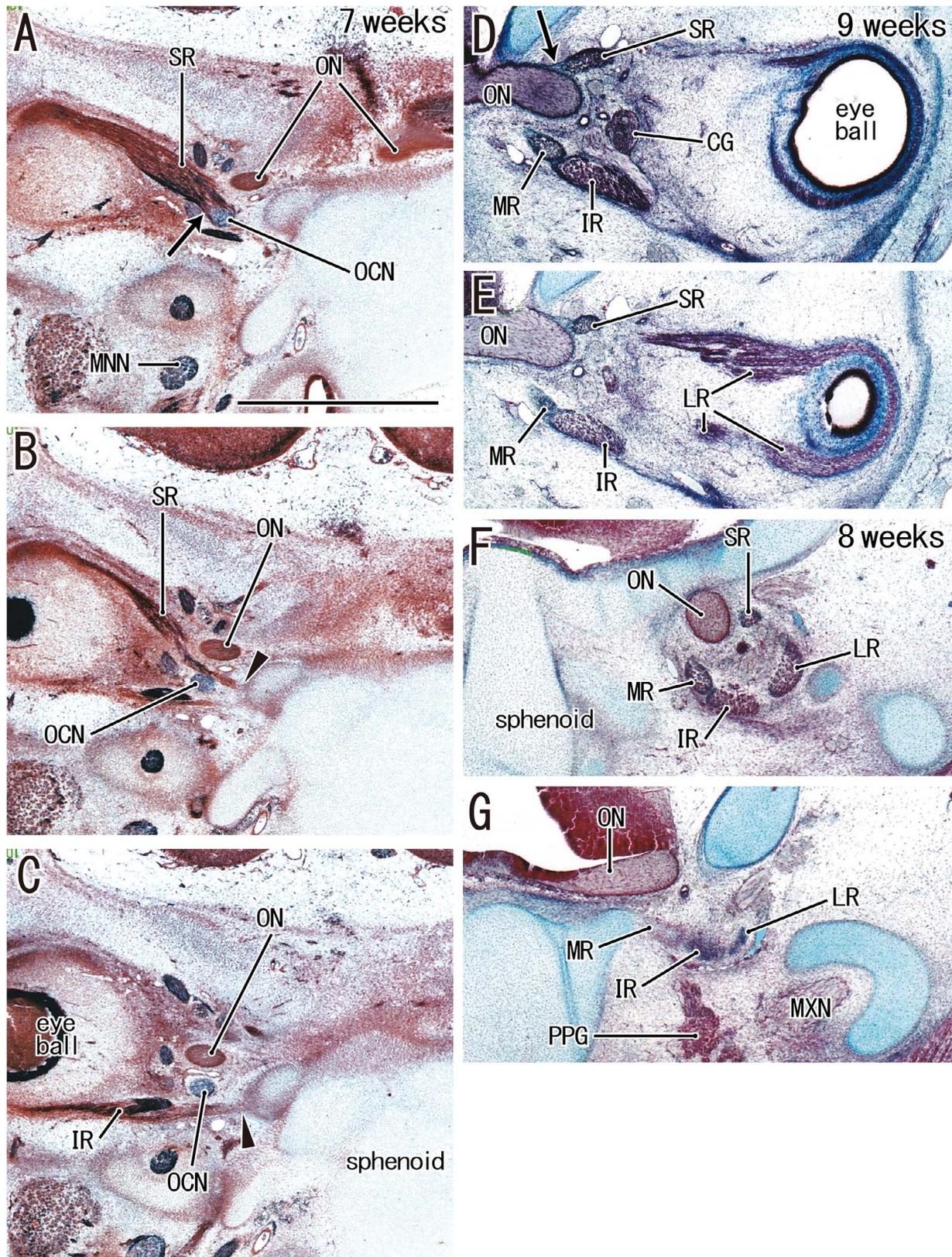
FIGURE 1. Early stage of rectus muscle origins at the orbital apex. Frontal sections. (**A–C**) Silver staining, an embryo of CRL 23 mm at approximately 7 weeks; (**D, E**) (azan staining), a fetus of CRL 38 mm at 9 weeks; (**F, G**) (azan staining), a fetus of CRL 29 mm at 8 weeks. (**A–E**) Longitudinal sections of rectus muscles because of lateral orientation of the eyeballs at the early stage; (**F, G**) cross-sections of the orbital apex due to plane tilting. Intervals between panels are 0.05 mm (**A–B, B–C**), 0.1 mm (**D–E**), and 0.4 mm (**F–G**). The SR and IR each carry a long tendon for the origin (*arrowheads* in **B** and **C**). To provide a temporal origin, the SR is tightly attached to the optic nerve (ON: *arrow* in **D**) or the oculomotor nerve (OCN: *arrow* in **A**). All panels were prepared at the same magnification (**A**, *scale bar*: 1 mm). ABN, abducens nerve; CG, ciliary ganglion; ICA, internal carotid artery; MXN, maxillary nerve; OPA, ophthalmic artery; ORM, orbitalis muscle; pet. sinus, petrosal sinus; PPG, pterygopalatine ganglion.
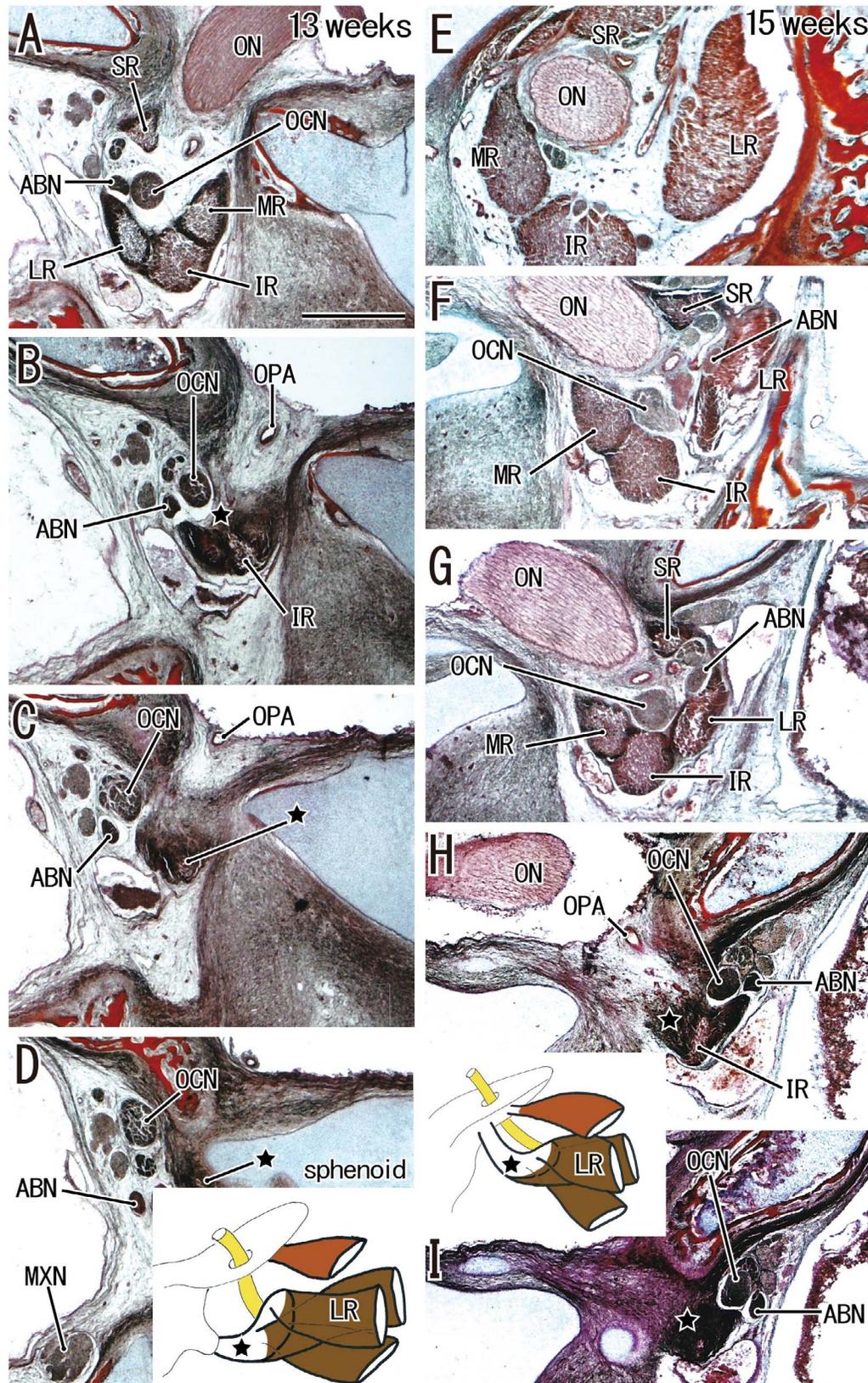
FIGURE 2. Orbital apex and rectus muscle origins at midterm: two fetuses. Frontal sections. HE staining. (**A–D**) A fetus of CRL 95 mm at approximately 13 weeks; (**E–I**) a fetus of CRL 113 mm at approximately 15 weeks. (**A, E**) The most anterior and (**D, I**) the most posterior sites in the specimen, respectively. Intervals between panels are 0.8 mm (**A–B**), 0.2 mm (**B–C**), 0.1 mm (**C–D**), 0.5 mm (**E–F**), 0.3 mm (**F–G**), 0.2 mm (**G–H**), and 0.05 mm (**H–I**). Schematic representation at the lower part of each column of panels exhibits a summary of muscle origins: the superior rectus, colored *red-brown* with a *star*, indicates a common tendinous origin of the other three recti. Being separated from the origin of the SR, a C-shaped arrangement of the LR, IR, and MR origins is evident in (**A**) and (**G**). The C-shaped common origin changes to a fibrous bundle (*star* in **C**, **D**, **H**, and **I**). All panels were prepared at the same magnification (**A**, *scale bar*: 1 mm).
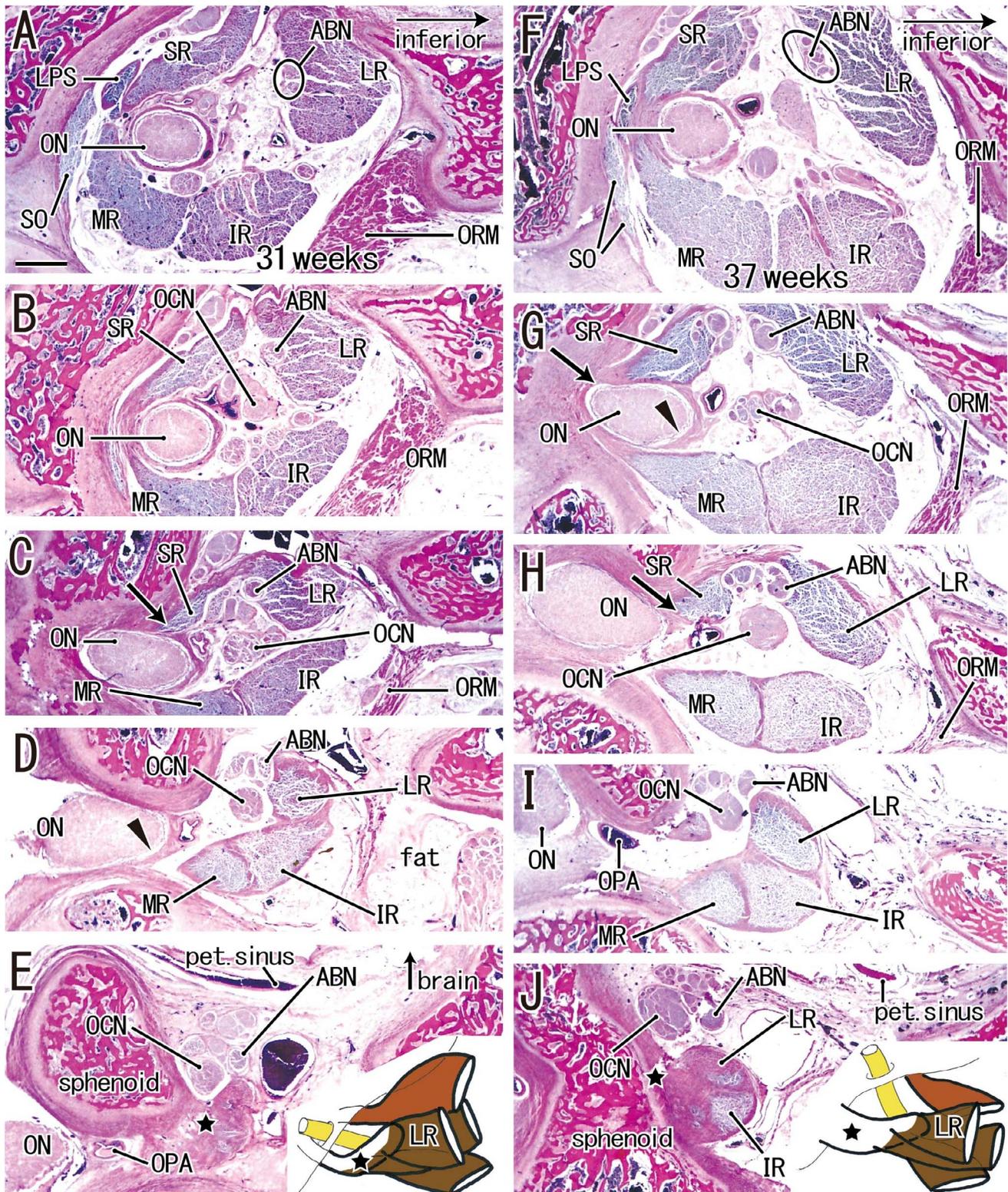
FIGURE 3. Orbital apex and rectus muscle origins near term: frontal sections from two fetuses. HE staining. (**A–E**) A fetus of CRL 264 mm at approximately 31 weeks; (**F–J**) a fetus of CRL 310 mm at approximately 37 weeks. (**A**) and (**F**) (or **E** and **J**) display the most anterior (or posterior) site in the specimen, respectively. Intervals between panels are 0.6 mm (**A–B, B–C, C–D, D–E**), 1.0 mm (**F–G**), and 0.5 mm (**G–H, H–I, I–J**). Schematic representation at the lower end of each column of panels exhibits a summary of muscle origins: the superior rectus, colored *red-brown* with a *star*, indicates a common tendinous origin of the other three recti. The C-shaped arrangement of the LR, IR, and MR origins can be seen in (**D**) and (**I**). The C-shaped common origin changes to a fibrous bundle (*star* in **E** and **J**). *Arrows* indicate the SR origin at the superomedial edge of the ON opening. *Arrowheads* indicate a dural sheath of the ON. All panels were prepared at the same magnification (**A**, *scale bar*: 1 mm).
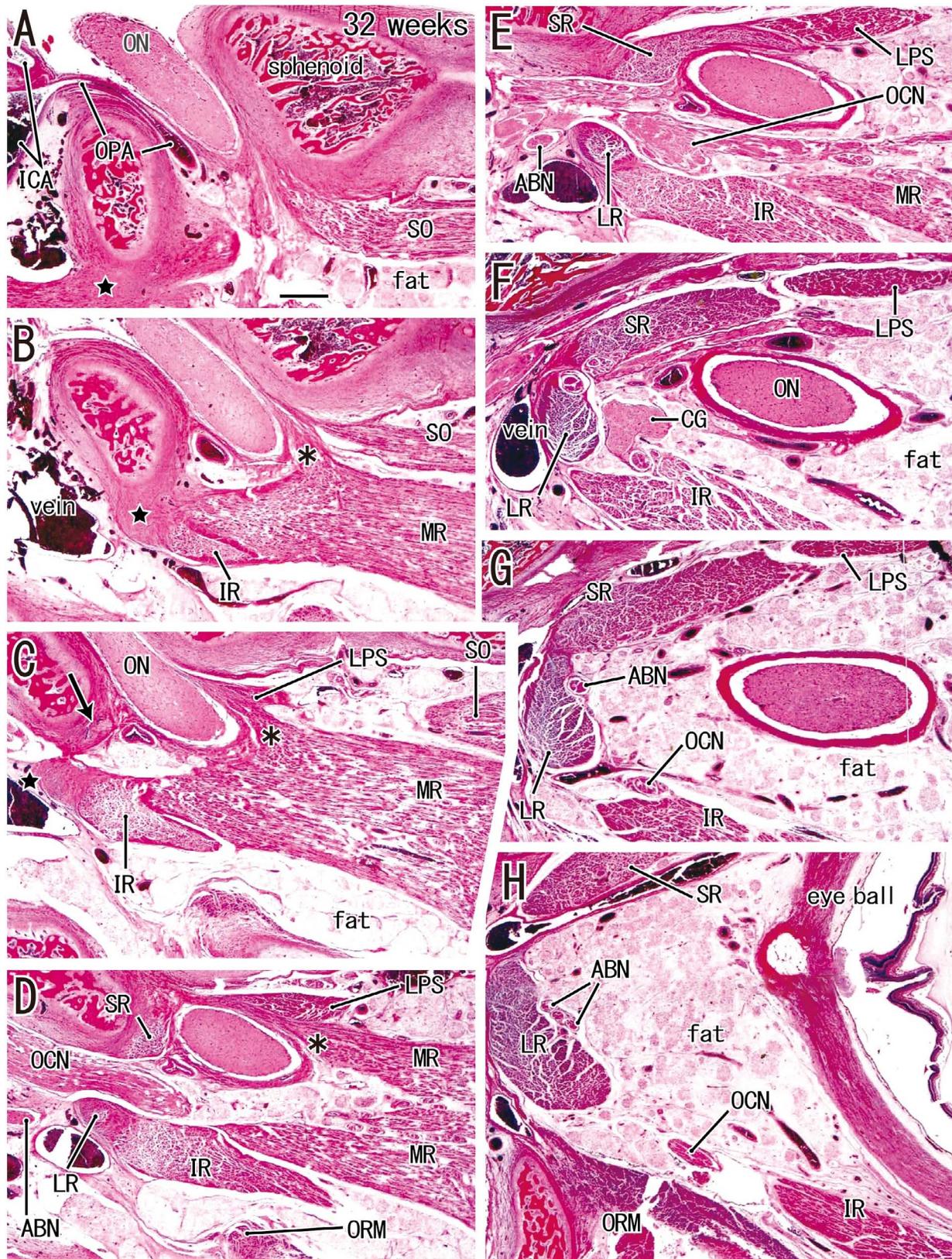
FIGURE 4. Orbital apex and rectus muscle origins near term: sagittal sections. A fetus of 272 mm at approximately 32 weeks. HE staining. The most medial (**A**) and lateral (**H**) sites in the specimen. Intervals between panels are 0.8 mm (**A–B**), 0.4 mm (**B–C, C–D**), 0.6 mm (**D–E**), 0.8 mm (**E–F, F–G**), and 1.6 mm (**G–H**). An additional head of the MR (*asterisk* in **B** and **C**) originates from the upper edge of the optic canal opening near the origins of the LPS and superior obliquus (SO). A common tendinous origin of the LR, IR, and MR (*stars* in **A–C**) is located posterior to the optic canal opening. All panels were prepared at the same magnification (*scale bar* in **A**, 1 mm).
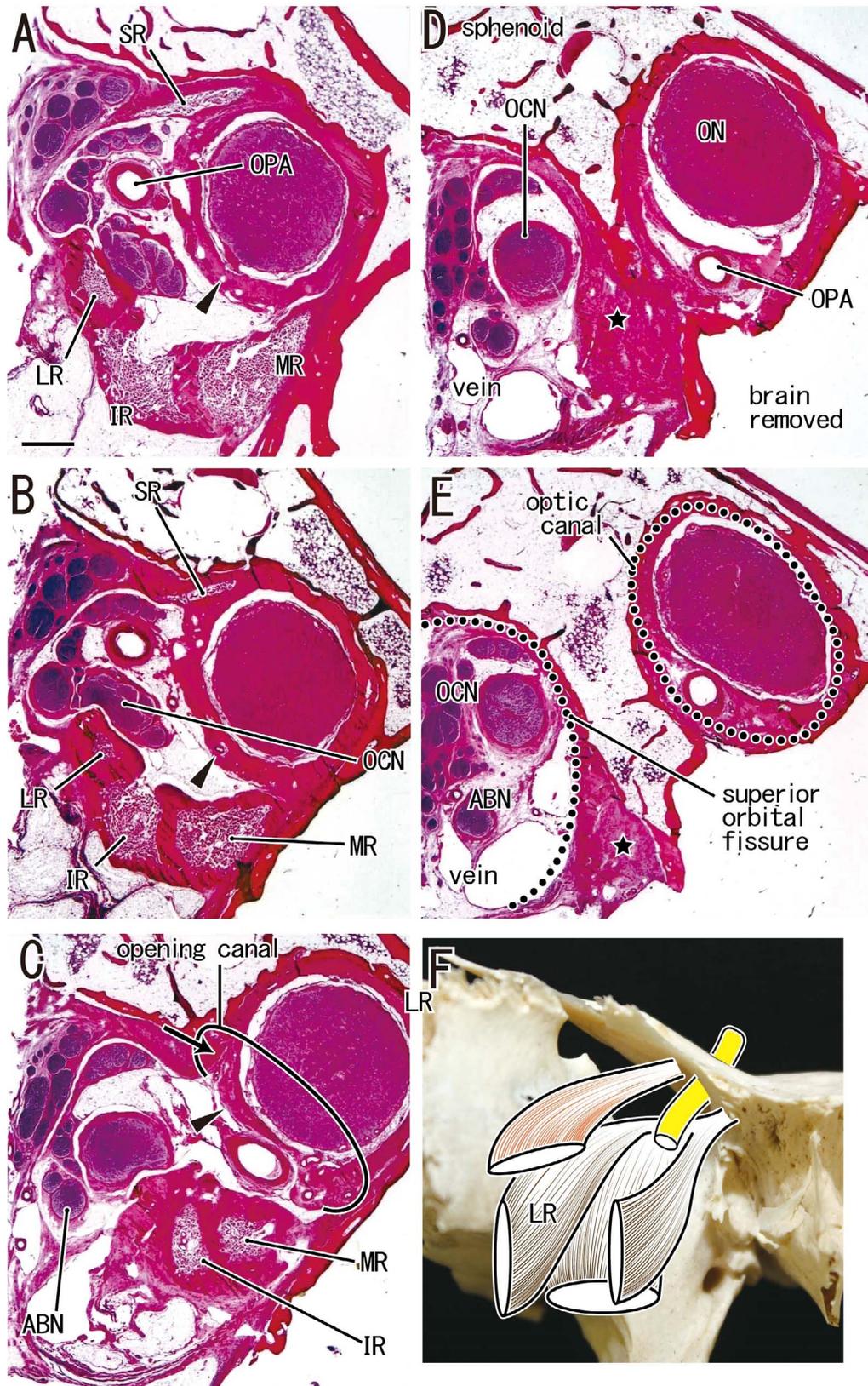
FIGURE 5. Orbital apex and rectus muscle origins in adults: frontal sections. Specimen from the cadaver of an 87-year-old male. HE staining. (**A**) (or **E**) displays the most anterior (or posterior) site in the specimen. Intervals between panels are 4.0 mm (**A–B**, **B–C**), 3.2 mm (**C–D**), and 2.8 mm (**D–E**). The C-shaped structure, representing the united origins of the LR, IR, and MR (**A** and **B**), is distant from the SR origin (*arrow* in **C**). The C-shaped common origin changes to a fibrous mass (*star* in **D** and **E**) and extends deeply into the superior orbital fissure. *Arrowhead* indicates the dural sheath of the ON, which is interrupted in (**C**). (**F**) (anterior view), projecting on a dry bone of another cadaver, exhibits the muscle arrangement schematically. The superior rectus is colored *red-brown*, whereas the other three recti are *dark brown*. (**A–F**) were prepared at the same magnification (*scale bar* in **A**: 1 mm).

However, this circular arrangement of muscles ended at a site 8.1 to 12.0 mm anterior to the optic canal opening. Separated from the SR origin at the anterosuperior edge of the optic canal opening (Figs. 5C, 5D), the LR, IR, and MR united to form a C-shaped muscle mass (Figs. 5B, 5C). The septa among these three rectus muscles became thicker in more posterior sections to form a thick tendinous bundle extending deeply into the superior orbital fissure (Figs. 5E, 5F). Sagittal sections revealed the common tendinous bundle extending posteriorly along a thin periosteum of the fissure to reach a site adjacent to the parasellar dura or petrosal sinus (Figs. 6A–C). The common tendon provided a notch at the surface of the abducens and/or oculomotor nerves (Figs. 6D, 6E). At the orbital apex, the LR was a fibrous bundle or tendon, and then more posteriorly a similar change occurred simultaneously in the IR and MR.

At the anterior edge of the optic canal opening, the optic nerve sheath opened at its inferior aspect to provide a passage for the ophthalmic artery (Fig. 5D). No histological connection was evident between the common tendinous origin of the three recti and the optic nerve sheath, and therefore the morphology was more appropriately described as "simple attachment." At the anteroposterior level including the posterior edge of the optic canal opening, all three rectus muscles fused into a common fibrous mass or bundle. The SR origin at the upper edge of the optic canal opening was located 2.0 to 3.5 mm superior to the common tendinous origin of the other three recti: this distance was determined mainly by the thickness of the optic nerve (3.0–4.5 mm). In contrast, the distance along the anteroposterior axis varied among adult individuals: 1.6 to 7.2 mm from the anteriorly located SR origin to the posterior common origin. Finally, at the orbital apex, the thicknesses of the nerves and muscles in adults were surprisingly similar to, or even a little smaller than those in specimens from near-term fetuses (Fig. 3 versus Fig. 5). The muscle fiber density appeared to be lower in adults, although we did not measure it.

DISCUSSION

Our present findings demonstrate that the MR, LR, and IR muscles take their origin from a C-shaped common tendon, whereas the superior rectus has an independent origin at the orbital apex, supporting the view that there is not a common tendinous ring supporting the origin of all four rectus muscles. Rather than specimens from adults (see Study Limitation below), those from fetuses near term provided a comprehensive understanding of the topographical relationship between the rectus muscle origins at the orbital apex. The results are summarized in Figure 7. Although the figure does not include all information from histological sections, it is quite different from current illustrations. Despite a literature search, we could find no published photos that show a tendinous annulus as the origin for all four rectus muscles. The description of a common tendon of origin may have resulted from the circular arrangement of the peripheral muscle bellies. The relatively recent clinical importance placed on the circularly arranged fascial structure connecting the peripheral muscle bellies of the rectus muscles, especially in connection with the concept of a pulley and sleeve system, might have encouraged belief in an "annular origin" of the extraocular recti in the absence of direct evidence at the orbital apex.

In their comprehensive review, Tawfik and Dutton[6] considered that a double origin of the LR might be plausible; however, we failed to find any double muscle slips or heads of the LR even in sagittal sections. In fact, it seems difficult to

visualize such double muscle slips in frontal sections, and indeed we found none for the MR in the present frontal sections. Because of the limited number of specimens available for sagittal sections in the present study, we could not rule out the possibility that double heads were carried by the LR in addition to the MR; however, it may have been an anomaly, as split muscles have been described during strabismus surgery.

Along the superomedial wall of the superior orbital fissure, the tendinous mass representing the common origin of the three recti (MR, IR, and LR) extended deeply toward the parasellar area. This morphology was noteworthy because it suggested a new area of clinical relevance. First, the thick common tendon of the three recti could interfere with the abducens nerve when it enters the orbit. In fact, the nerve showed inferior angulation immediately posterior to the tendon. Although this nerve course has been of major interest to neurosurgeons (as reviewed by Joo et al.[9]), the possibility of a functionally important tendinous bundle approaching the parasellar area has not been considered. Second, because the common tendon was thick and long in the superior orbital fissure, it is in danger of injury during a lateral orbitotomy approach for removal of tumors in the middle cranial fossa or cavernous sinus.[10-12] Third, ophthalmic veins appeared to avoid the thick common tendon when draining from the orbit. In radiologic evaluations of orbital apex syndrome,[13-15] it appears that no one has yet discriminated the tendon from the periosteum extending along the orbital fissure. Fourth, notably, in addition to this tendinous origin, we found that parts of the SR and/or LR fibers originated from the optic or oculomotor nerve sheath (Figs. 1A, 1D). We regarded that this probably represented a temporal or transitory origin appearing at a short period of fetal development.

Study Limitations

First, it was difficult to find good early-stage sections because of tilting of the sectional planes. Likewise, specimens from near-term fetuses are difficult to obtain, not only in Japan but elsewhere. Rather than using fetal specimens, we are now preparing a further study using a larger number of adult cadavers. Second, sections of specimens taken from elderly adults did not include all of the bony elements at and around the orbital apex, and only parts of the sphenoid. Therefore, the topographical anatomy at and along the superior orbital fissure might not have been well demonstrated. For further study, it would be important to obtain larger tissue blocks from intact cadaver orbits. Third, although it might be out of focus, the present study showed individual variations in several morphologies: (1) a site of origin of a common tendon of three recti, (2) a site of origin of the SR, and (3) an additional slip of the MR; thus, we wish to find the individual variation between more specimens of almost the same age.
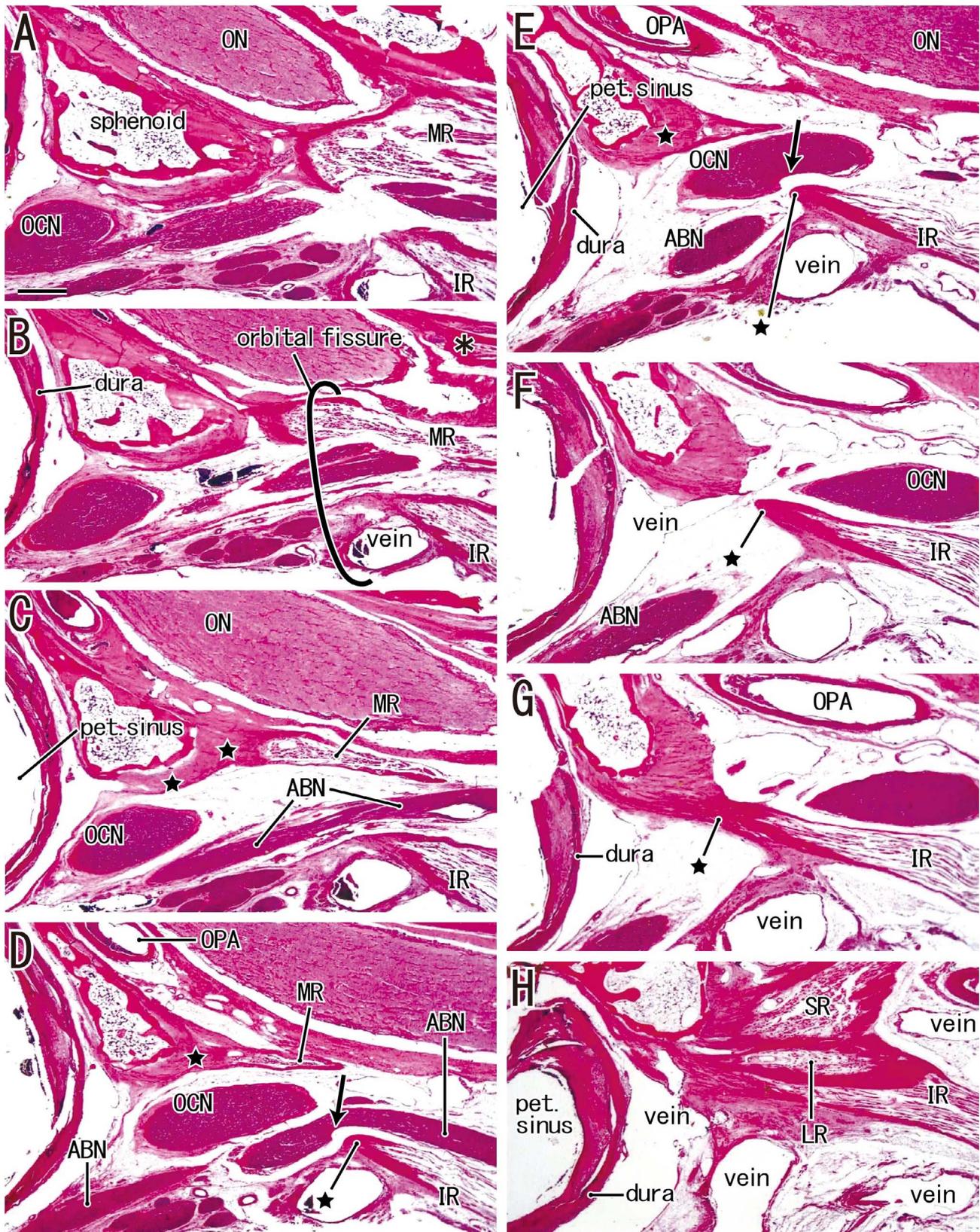
FIGURE 6. Orbital apex and rectus muscle origins in adults: sagittal sections. Specimen from the cadaver of an 89-year-old female. HE staining. (**A**) (or **H**) displays the most medial (or lateral) site in the specimen. Intervals between panels are 0.8 mm (**A–B**, **B–C**), 1.6 mm (**C–D**), 1.2 mm (**D–E**), 1.6 mm (**E–F**), 0.4 mm (**F–G**), and 2.5 mm (**G–H**). Because of the additional head (*asterisk* in **B**), the MR appears to cover the opening of the optic canal (**A**). A tendinous band (*stars*) receives the MR in (**C**) and (**D**), the IR in (**F**) and (**G**), and the LR in (**H**). Note the petrosal sinus and dura adjacent to the posterior opening of the orbital fissure. The band provides a notch at a surface of the abducens and oculomotor nerves, respectively (*arrow* in **D** and **E**). All panels were prepared at the same magnification (*scale bar* in **A**: 1 mm).
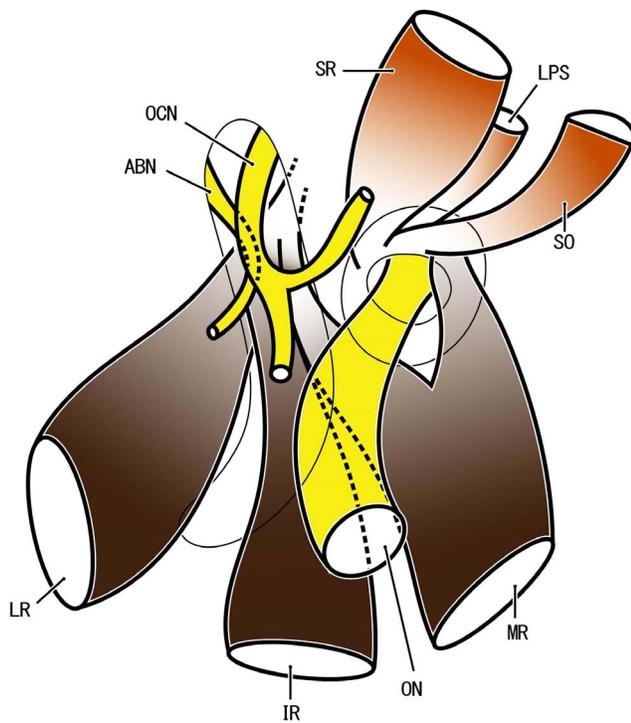
FIGURE 7. Summary of the present observations. The SR, LPS, SO, and an additional head of the MR (*red-brown*) originated from the upper edge of the optic canal opening, but the topographical relationships among these origins are not well shown because of draftsmanship limitations. The additional head is drawn thicker than the actual one for emphasis. The other three rectus muscles (MR, IR, and LR; *dark brown*) become united to form a common tendon extending deeply into the superior orbital fissure. *Brown colors* indicate the respective areas of striated muscle fibers: thus, (1) the origins of the LPS, SO, and the MR additional head had no definite tendon but muscular; (2) LR muscle fibers ended anterior to the MR and IR.

References

1. Morris H. *Morris' Human Anatomy*. Vol. 11. Philadelphia, PA: Blakiston; 1953:1248.

2. Koornneef L. The development of the connective tissue in the human orbit. *Acta Morphol Neerl Scand*. 1976;14:263–290.

3. Koornneef L. New insights in the human orbital connective tissue. *Arch Ophthalmol*. 1977;95:1269–1273.

4. Sevel D. The origins and insertions of the extraocular muscles: development, histologic features, and clinical significance. *Trans Am Ophthalmol Soc*. 1986;84:488.

5. Kahkeshani K, Ward PJ. Connection between the spinal dura mater and suboccipital musculature: evidence for the myodural bridge and a route for its dissection—a review. *Clin Anat*. 2012;25:415–422.

6. Tawfik HA, Dutton JJ. Embryologic and fetal development of the human orbit. *Ophthalmic Plast Reconstr Surg*. 2018;34: 405–421.

7. Naito M, Suzuki R, Abe H, Rodriguez-Vazquez JF, Murakami G, Aizawa S. Fetal development of the human obturator internus muscle with special reference to the tendon and pulley. *Anat Rec (Hoboken)*. 2015;298:1282–1293.

8. Katori Y, Hyun Kim J, Rodríguez-Vázquez JF, Kawase T, Murakami G, Hwan Cho B. Early fetal development of the intermediate tendon of the human digastricus and omohyoideus muscles: a critical difference in histogenesis. *Clin Anat*. 2011;24:843–852.

9. Joo W, Yoshioka F, Funaki T, Rhoton AL Jr. Microsurgical anatomy of the abducens nerve. *Clin Anat*. 2012;25:1030–1042.

10. Grassi P, Strianese D, Mariniello G, Bonavolontà G. Delayed recovery of visual acuity after sphenoorbital meningioma surgical removal: case report and review of the literature. Is visual acuity recovery possible after an initial decline? *J Neurol Surg A Cent Eur Neurosurg*. 2015;76:328–331.

11. Ulutas M, Boyacı S, Akakın A, Kılıç T, Aksoy K. Surgical anatomy of the cavernous sinus, superior orbital fissure, and orbital apex via a lateral orbitotomy approach: a cadaveric anatomical study. *Acta Neurochir (Wien)*. 2016;158:2135–2148.

12. Alzhrani GA, Gozal YM, Sherrod BA, Couldwell WT. A modified lateral orbitotomy approach to the superior orbital fissure: a video case report and review of anatomy. *Oper Neurosurg (Hagerstown)*. 2019;16:685–691.

13. Ikawa F, Uozumi T, Kiya K, Arita K, Kurisu K, Harada K. Cavernous sinus meningioma presenting as orbital apex syndrome. Diagnostic methods of dynamic MRI, spoiled GRASS (SPGR) image. *Neurosurg Rev*. 1995;18:277–280.

14. Imaizumi A, Ishida K, Ishikawa Y, Nakayoshi I. Successful treatment of the traumatic orbital apex syndrome due to direct bone compression. *Craniomaxillofac Trauma Reconstr*. 2014;7:318–322.

15. Jin H, Gong S, Han K, et al. Clinical management of traumatic superior orbital fissure and orbital apex syndromes. *Clin Neurol Neurosurg*. 2018;165:50–54.